Variables influencing the neural correlates of perceived risk of physical harm

Mariam Coaster · Baxter P. Rogers · Owen D. Jones ·
W. Kip Viscusi · Kristen L. Merkle · David H. Zald ·
John C. Gore

Abstract Many human activities involve a risk of physical harm. However, not much is known about the specific brain regions involved in decision making regarding these risks. To explore the neural correlates of risk perception for physical harms, 19 participants took part in an event-related fMRI study while rating risky activities. The scenarios varied in level of potential harm (e.g., paralysis vs. stubbed toe), likelihood of injury (e.g., 1 chance in 100 vs. 1 chance in 1,000), and format (frequency vs. probability). Networks of brain regions were responsive to different aspects of risk information. Cortical language- processing areas, the middle temporal gyrus, and a region around the bed nucleus of stria terminalis responded more strongly to high- harm conditions. Prefrontal areas, along with subcortical ventral striatum, responded preferentially to high-likelihood conditions. Participants rated identical risks to be greater when information was presented in frequency format rather than probability format. These findings indicate that risk assessments for physical harm engage a broad network of brain regions that are sensitive to the severity of harm, the likelihood of risk, and the framing of risk information.

Keywords Decision-making · Risk prefrontal cortex

Introduction

Many human activities involve physical risks. People make decisions about such activities based on the perceived benefit or penalty of the outcome and the probability of the potential harm. In standard economic theory, a risky choice involves different possible outcomes, each of which has an associated probability. To make a risky decision, a reason-

M. Coaster · D. H. Zald · J. C. Gore
Vanderbilt Neuroscience, Vanderbilt University,
Nashville, Tennessee, USA

M. Coaster · B. P. Rogers · K. L. Merkle · J. C. Gore
Vanderbilt University Institute of Imaging Science,
Vanderbilt University,
Nashville, Tennessee, USA

B. P. Rogers · J. C. Gore
Department of Radiology and Radiological Sciences,
Vanderbilt University,
Nashville, Tennessee, USA

O. D. Jones
Vanderbilt Law School and Department of Biological Sciences,
Vanderbilt University,
Nashville, Tennessee, USA

W. K. Viscusi
Vanderbilt Law School, Department of Economics,
and Owen School of Management, Vanderbilt University,
Nashville, Tennessee, USA

D. H. Zald
Vanderbilt Department of Psychology, Vanderbilt University,
Nashville, Tennessee, USA

B. P. Rogers · J. C. Gore
Department of Biomedical Engineering, Vanderbilt University,
Nashville, Tennessee, USA

M. Coaster (✉)
Vanderbilt University Institute of Imaging Science
and Vanderbilt Neuroscience Program,
1161 21st Avenue South, Medical Center North, AA1101,
Nashville, Tennessee 37232, USA
e-mail: mariam.coaster@vanderbilt.edu

ing individual assesses the pertinent probabilities, evaluates the different possible outcomes, and determines the overall attractiveness of the risky prospect. A substantial literature has documented the difficulty people have in making risky decisions in a consistent manner and in a way that conforms with rational norms (Kahneman & Tversky, 1979).

The neuroimaging literature on risk has usually examined decisions in the context of monetary rewards and losses. A network of brain regions is engaged during the perception and evaluation of risk involving monetary payoffs, including the caudate nucleus, which is involved in calculating the magnitude of gain or loss of a choice (Hsu, Bhatt, Adolphs, Tranel, & Camerer, 2005), and limbic regions comprising the orbitofrontal cortex (OFC), amygdala, ventromedial prefrontal cortex, and insular cortex, thought to be recruited for the assessment of reward probability or outcome uncertainty (Hsu et al., 2005; Tobler, O'Doherty, Dolan, & Schultz, 2007; Walton, Croxson, Behrens, Kennerley, & Rushworth, 2007). In addition, different parts of the prefrontal cortex have been associated with risk aversion and risk seeking as the expected value of monetary reward becomes differentially coded with uncertainty (statistical variance), depending on the individual differences in the risk attitudes of participants (Tobler et al., 2007). The anterior cingulate cortex, in particular, appears involved in mediating choice conflicts during financial risk-taking (Kuhnen & Knutson, 2005).

Unlike monetary payoffs or rewards involving physical objects, physical harms pose additional challenges for valuation. Severe harms, such as death and disabling injuries, affect one's well-being in an irreversible manner and determine the utility one can derive from other aspects of one's life (Viscusi & Evans, 1990). In the context of reading words that imply physical risk information, Vorhold et al. (2007) showed that risk rating engaged the left medial prefrontal cortex, left inferior frontal gyrus, and left amygdala. This suggests that certain brain areas are particularly sensitive to processing the qualitative and subjective aspects of risk information. Evolutionarily, the perception of the risk of harmful physical consequences has also been shown to engage flight or fight physiological responses through the amygdala and connected limbic areas (Phillips & LeDoux, 1992). This suggests that the underlying neural substrates involved in the perception and assessment of risk involving physical harm may include limbic and paralimbic pathways. However, such neural substrates engaged during the evaluation of risks associated with physical harms have yet to be elucidated.

In addition, there are both empirical and theoretical reasons to postulate that variations in the format of communicating probabilities can differentially affect both neural processes and behavior, even for probabilities that are statistically equivalent. For example, behavioral studies on risk perception have shown that individuals understand and process probability information differently when probability information is communicated in a frequency format (for example, *20 out of 100*) versus what has been termed a probability format, using a decimal (e.g., *.20*) or a percentage (e.g., *20%*). The frequency format provides a reference class that enables people to conceptualize more exemplars of the risk outcomes, whereas the probability format is more abstract. Participants in a study by Yamagishi (1997) rated a disease that kills 1,286 people out of every 10,000 as being more dangerous than one that kills 24.14% of the population, even though 24.14% is almost twice as great a risk. Another report found that participants who were presented with a high probability of harm in the frequency format were willing to pay a higher price for improved medication as compared to participants who received the same information in the probability format (Siegrist, 1997). Moreover, Slovic and colleagues (Slovic, Monahan, & MacGregor, 2000) found that forensic psychologists and psychiatrists rated the risk of a patient committing a violent crime after discharging them from a mental health unit as being greater in the frequency format (*20 out of 100 people like X will commit a given crime*) than when the equivalent risk was presented in the probability format (*X has 20% chance of committing a crime*). Based on a series of jury studies, Koehler (2001) concluded that the frequency format was more readily understood than the probability format for processing of statistical information such as DNA statistics. Even when the frequency information format implies the same probability values as does the probability format, these studies suggest that people process frequencies and probabilities differently, in ways that often affect behavior. Some hypothesize that this difference arises because frequency distributions are the more natural format in which risks are perceived in the world around us, which would suggest that the human brain evolved to assess those formats more easily and intuitively (Gigerenzer, 1998), which may in turn lead to systematic errors in risk perception between formats (Jones & Goldsmith, 2005).

The present study seeks to lay a broader foundation for understanding the neural processing of risk in the context of physical activities, and to determine the impact of several important variables that may generate differences in such processing. Specifically, the present study uses functional magnetic resonance imaging (fMRI) to investigate the neural signatures underlying risk assessment in relation to aversive outcomes (personal physical harms), while varying the severity of harm, the likelihood of harm, and the format in which likelihoods are expressed. As participants in our study rated the severity of the risk of continuing to engage in a risky activity, we hypothesized that limbic brain regions would be sensitive to the qualitative information in risk scenarios (severity of harm), while more frontal and association areas would be sensitive to the quantitative (likelihood of harm) aspects of risk.

Method

Participants

A group of 21 healthy participants completed the study. Of these participants, 19 were included in the fMRI data analysis (11 males, 20–28 years of age; 8 females, 20–29 years of age) on the basis of consistent behavioral performance and maximal head motion of less than one voxel (2.75 mm^3). All participants gave written informed consent for the study as approved by the Institutional Review Board of Vanderbilt University Medical Center. Participants received $75 for their participation.

fMRI data acquisition

Images were acquired using a Philips 3-T Achieva (Philips Healthcare). Whole-brain three-dimensional anatomical scans were acquired using a T1-weighted turbo field echo pulse sequence. A total of 170 slices were collected in coronal orientation with a field of view (FOV) of 256 × 256 × 170 mm, a 256 × 256 × 170 reconstruction matrix, SENSE factor of 2, scan duration of 6 min 31 s, repetition time (TR) of 8.077 ms, echo time (TE) of 3.67 ms, and a voxel resolution of 1 × 1 × 1 mm, with zero gap and a flip angle (FA) of 5°. This high-resolution structural scan was used to aid in normalization and co-registration of the functional data.

Whole-brain blood oxygen level dependent (BOLD) images were acquired using a T2*-weighted echoplanar imaging sequence. A total of 40 slices were collected in the axial orientation, aligned parallel to the AC–PC axis, covering cortical and subcortical regions with FOV of 220 × 119 × 220 mm; 80 × 80 reconstruction matrix, SENSE factor of 1.8, TR of 2 s, TE of 25 ms, and a voxel resolution of 2.75 × 2.75 × 2.75 mm, with a 0.25-mm gap and an FA of 79°. Image volumes were acquired in runs of duration 7 min 19 s, with 212 volumes per run. Participants completed a slow event-related fMRI design with eight runs. The onset of each run
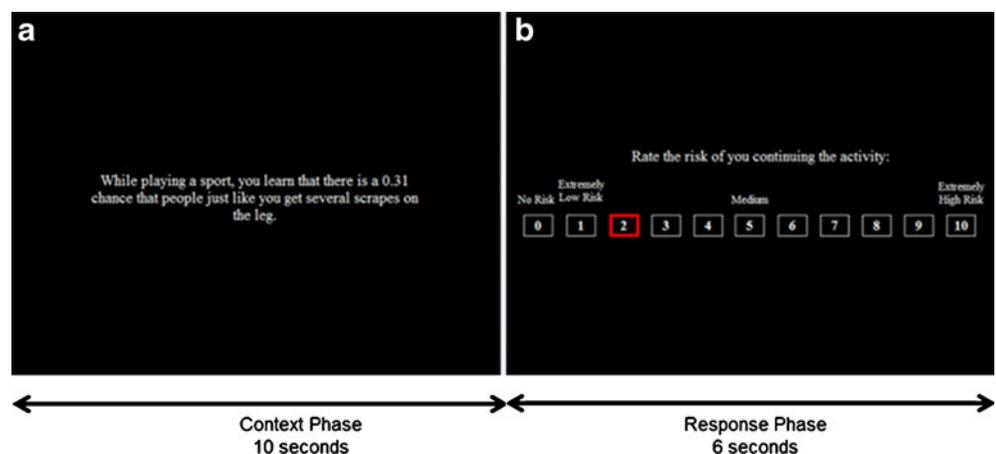
was triggered from the scanner so that the fMRI data collection and stimulus presentation were synchronized.

Experimental design

Each run in the experimental paradigm comprised 16 trials interleaved with a variable interstimulus interval (ISI, 8–16 s). Each trial was divided into two phases: context and response (Fig. 1A, B). In the context phase, the participants were presented with a textual scenario (average of 45 words in length) for 10 s (Fig. 1A). The text appeared on a black screen and subtended a visual angle of 15°–20°. The scenarios were chosen pseudorandomly from a pool of 128 unique scenarios, of which 64 were in the probability format and 64 in the frequency format. The 64 scenarios in each format were further divided into two levels of risk (high and low) and two levels of harm (high and low). The pseudorandomization minimized the possibility that a scenario with the frequency format and an equivalent probability format would be presented one after the other. Furthermore, a scenario in the frequency format and its equivalent scenario in the probability format never appeared in the same run, removing instances of back-to-back repetition. The frequency and probability formats were equivalent in their likelihoods of risk, as well as the severity of harm. In addition, the order of the eight runs was randomly presented across the participants. Participants were naive to all stimuli.

The 10-s context phase was followed by a 6-s response phase, during which the participant had to rate the risk of engaging in a physical activity on a numerical scale from 0 to 10 (Fig. 1B). Participants were given a trackball mouse to use to click inside one of the response option boxes. The response box options varied from 0 (no risk) and 1 (extremely low risk) to 10 (extremely high risk). The participants were instructed to rate the severity of the risk of continuing to engage in a physical activity that they had read about in the context phase. The response option box would turn red once a response was

Fig. 1 Sample stimulus screen. (a) Context phase: Scenario. Example: "While playing a sport, you learn that there is a 0.31 chance that people just like you get several scrapes on the leg." (b) Response phase. Participants viewed the following instruction: "Rate the risk of you continuing the activity" and they were given a choice from 0 to 10. 0 represented "No risk"; 1 represented "Extremely low risk"; 5 represented "Medium" risk and 10 represented "Extremely high risk"

made, giving participants feedback that the buttonpress was successful.

The task was presented using E-Prime Professional software (Version 2.0: Psychology Software Tools Inc.). Before beginning the experimental runs, the participants completed a 5-min practice session outside the scanner and a 5-min practice session inside the scanner. This allowed the participants to assimilate themselves to the task and become familiar with using the trackball mouse inside the scanner. The practice sessions included viewing 16 scenarios split evenly between frequency and probability formats.

The scenarios presented aversive outcomes involving injury while engaging in a physical activity. The scenarios varied by the level of the risk probability (high or low risk) and the associated level of harm (high or low harm). The likelihood of risk varied between a 1-in-1,000 chance of getting hurt (low risk) to a 1-in-100 chance of getting hurt (high risk). The severity of the harm varied from minor injuries (low harm: scrapes on the skin) to more serious or even fatal injuries (high harm: broken bones, death). The classification of harm as low or high was established in a separate behavioral study with 20 participants who rated the harm level from low to high for 128 distinct injuries. The classification of the levels of risk was conducted in another behavioral study with 19 participants who evaluated harm-related scenarios, with the probability of a risky outcome ranging from low (1 in 10,000) to medium (1 in 1,000) to high (1 in 100). For the present study, only the low-probability and high-probability risk scenarios were used, because participants showed a clear distinction in their ratings between these two categories of risk.

The range of physical activities in the present study included playing a sport, driving down a dirt road, helping a friend with a house project, and hiking. The participants were advised not to rate how likely they were to participate in the activity or how likely they were to incur the injury. Instead, they were to rate the risk of continuing an activity if they were already participating in it, based on the risk information presented in the scenario. There was no instruction given on how the participants were supposed to interpret the likelihood of risks in the different formats. Most reported that they converted the ratio and the decimal format to a percentage number. Anecdotally, from post-experimental briefing sessions with the participants, they recounted that the assessment of risk in each scenario involved combining the probability of risk and the associated harm to make a judgment about the rating of risk in an activity.

fMRI data analysis

Functional images were corrected for participants' head motion, slice time corrected, and normalized into a standard stereotaxic space (MNI) for intersubject comparisons using SPM5 (Wellcome Department of Cognitive Neurology, London, U.K.). A smoothing filter 8 mm in width was applied after normalization.

A general linear regression model was used to analyze the fMRI data. From the overall time series, we defined epochs that were time-locked to the onset of the context phase for every scenario. Each epoch lasted for the entire duration of the context phase and the response phase, until the participant pressed a button to indicate a response. Every epoch thus represented a regressor that combined both the context and response phases of the scenario. Eight different regressors were created for each run, with each regressor representing a unique trial type as indicated in the factorial design. These regressors included: frequency low risk–low harm, frequency low risk–high harm, frequency high risk–low harm, frequency high risk–high harm, probability low risk–low harm, probability low risk–high harm, probability high risk–low harm, and probability high risk–high harm.

The average parameter estimates of the eight regressors were included in a second-level random-effects analysis. In this analysis, we examined the main effects and interactions of each of the factors—Format, Risk, and Harm in a model analogous to a voxelwise repeated measures $2 \times 2 \times 2$ ANOVA. We performed two separate analyses using different voxel-level thresholds of $p < .001$ and $.005$. All clusters that were significant at $p < .05$, corrected for multiple voxel comparisons based on cluster extent, are reported. The initial analysis used a cluster-defining voxel-level threshold of $p < .001$ and an $1,864$-mm^3 minimum cluster size. A second analysis, performed post hoc, used a voxel threshold of $p < .005$ and a $4,440$-mm^3 minimum cluster size, and revealed additional clusters. This dual approach provided a balance in the ability to detect both large-magnitude but small-volume foci and effects of more modest magnitude but larger volume. For completeness, we present all results at both thresholds, along with their corrected p values. Only the main effect and interaction effect contrast maps that passed significance at the whole-brain level are reported in this article. As a convention through the text, we use the term *risk conditions* to refer to the likelihood or probability of risk associated with a physical activity, and *harm conditions* to refer to the severity of the harm associated with physical injury in an activity. Additionally, *risk rating* refers to the behavioral ratings of participants while evaluating the risk of continuing to engage in a physical activity.

Results

Behavioral results

Behavioral responses were collected during the entire duration of the scan and analyzed as a within-subjects

three-way repeated measures ANOVA across 21 participants in SPSS (Version 17). Main effects of format, harm, and risk were observed. Within the main effect of format, the frequency condition had a significantly higher marginal mean rating, as compared to the probability condition (Hotelling's Trace Test, $F = 5.861$, degrees of freedom = 20, $p < .025$, $N = 21$). For the main effect of risk, the high-risk condition had a significantly higher marginal mean rating, as compared to low-risk conditions (Hotelling's Trace Test, $F = 182.4$, degrees of freedom = 20, $p < .001$, $N = 21$). Similarly, for the main effect of harm, the high-harm conditions showed higher marginal mean ratings as compared to the low-harm conditions (Hotelling's Trace Test, $F = 250.0$, degrees of freedom = 20, $p < .001$, $N = 21$). A Harm x Risk interaction was also observed, with a significant difference between high and low risk in the high-harm condition as compared to the low-harm condition (Hotelling's Trace Test, $F = 111.6$, degrees of freedom = 20, $p < .001$, $N = 21$; see Fig. 2).

Reaction time differences across conditions Since our paradigm entailed two distinct phases of processing (context and response), we also examined the influence of reaction time differences across conditions. In a within-subjects three-way repeated measure ANOVA across 21 participants in SPSS, we observed a main effect of harm, where participants took longer to respond in high-harm as compared to low-harm conditions (Hotelling's Trace test, $F = 5.158$, degrees of freedom = 20, $p < .034$, $N = 21$). Similarly, a trend toward significance was observed in the risk condition, with high-risk conditions producing longer reaction times than low-risk conditions. We also measured reaction time data over the course of each run to determine whether they became faster as the participants did more trials. We did not see a significant change over time, suggesting that each scenario was treated uniquely, with
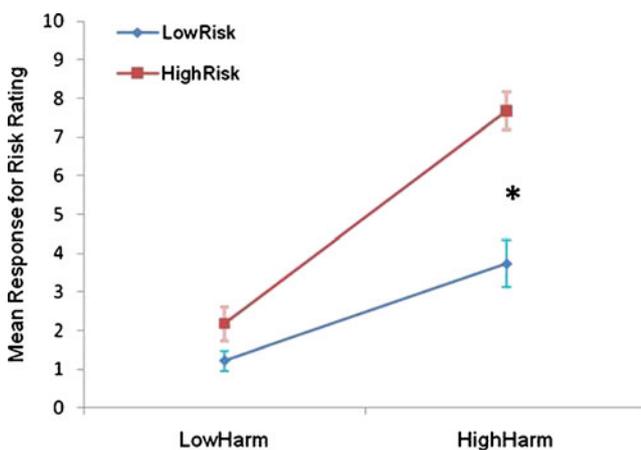

Fig. 2 Harm x Risk interaction plot of risk ratings as observed in the three-way repeated measures ANOVA across participants. *Significant difference between high and low risk in the high-harm condition (Hotelling's Trace Test, $F = 111.6$, degrees of freedom = 20, $p < .001$, $N = 21$)

participants varying in their decision-making reaction time depending on the condition presented.

fMRI whole-brain results

The fMRI data were analyzed using a factorial design with three levels (format, harm, and risk). Main effects of harm and risk were observed in the high-harm and high-risk conditions, respectively. A main effect of format was not observed in this study. However, interaction effects were noted for high-harm and high-risk conditions within the frequency and probability formats separately.

Main effect and interaction effects of harm: Average BOLD response for the high-harm as compared to the low-harm conditions For the main effect of harm collapsed across formats and risk, high-harm scenarios activated a group of subcortical and cortical brain regions (Table 1). Subcortically, the right bed nucleus of the stria terminalis (BNST) showed preferential BOLD activation in the high-harm conditions, as compared to low-harm conditions (Fig. 3).

Cortically, the language-processing areas such as the middle temporal gyrus (MTG), inferior frontal gyrus (IFG), and angular gyrus (AG) were recruited for high-harm conditions in comparison to the low-harm conditions (Figs. 4 and 5). For the main effect of harm where low-harm conditions were compared to high-harm conditions, the right parietal operculum responded preferentially.

Many of the same brain regions that showed a main effect of harm showed responses that demonstrated a harm x format interaction, in which the frequency format for high-harm conditions demonstrated strong activations (Table 1). BOLD activity within the left frontal pole was observed for this interaction. Within the probability format, the high-harm conditions engaged the visual cortex and subcortical ventral lateral and ventral anterior thalamic nuclei. Moreover, within the probability format, areas of the paracentral lobule and the visual cortex showed an interaction effect in low-harm as compared to high-harm conditions (Table 2). There were no significant brain regions activated in the frequency format for low-harm conditions.

Main effect and interaction effects of risk: Average BOLD response for the high-risk as compared to the low-risk conditions For the main effect of risk, high-risk as compared to low-risk conditions recruited a broad, prefrontal BOLD response, irrespective of the harm level and the format of presentation (Table 3). More specifically, the ventrolateral prefrontal cortex (VLPFC) (Fig. 6), the presupplementary motor area (preSMA) (Fig. 7), and an area within the middle/superior frontal

Table 1 Brain regions showing greater average BOLD response for high-harm as compared to low-harm conditions

Region	Hemisphere	MNI Space Coordinates			Number of Activated Voxels	t (peak voxel)	p (voxel level)	p (whole brain)
		x	y	z				
High Harm > Low Harm								
BNST	R	10	2	–2	253	4.42	p < .001	p ≤ .029
Middle temporal gyrus	L	–54	–34	–4	234	4.69	p < .001	p ≤ .038
Angular gyrus	R	32	–62	36	625	4.50	p < .001	p ≤ .001
Lateral visual cortex	L	–32	–86	–10	433	4.92	p < .001	p ≤ .002
Visual cortex	R	12	–78	–6	1,047	7.17	p < .001	p < .001
Middle frontal gyrus	R	40	30	20	247	4.63	p < .001	p ≤ .031
Parieto-occipital junction	L	–32	–72	34	606	3.72	p < .005	p ≤ .025
IFG pars opercularis	L	–40	10	28	913	4.21	p < .005	p ≤ .003
Frequency High Harm > Low Harm								
BNST	R	10	2	–2	405	4.65	p < .001	p ≤ .003
Middle temporal gyrus	L	–54	–34	–4	396	4.37	p < .001	p ≤ .004
Angular gyrus	R	32	–62	36	818	4.85	p < .001	p < .001
Visual cortex	R	12	–76	–6	1,091	6.60	p < .001	p < .001
Parieto-occipital junction	L	–32	–72	38	436	4.55	p < .001	p ≤ .002
Middle frontal gyrus	R	54	30	28	514	4.97	p < .001	p ≤ .001
Frontal pole	L	–22	68	10	222	4.28	p < .001	p ≤ .046
IFG pars opercularis	L	–40	10	28	624	5.09	p < .001	p < .001
Inferior visual cortex	L	–30	–86	–10	1,053	4.20	p < .005	p ≤ .001
Probability High Harm > Low Harm								
Visual cortex	R	12	–78	–6	356	5.06	p < .001	p ≤ .007
Thalamus: Ventral lateral/Ventral anterior nucleus	L	–10	–12	0	509	4.51	p < .005	p ≤ .053

The number of activated voxels shown is based on a cluster-wise thresholding criterion for each voxel, corrected for multiple comparisons across the whole brain. BNST, bed nucleus of the stria terminalis; IFG, inferior frontal gyrus.
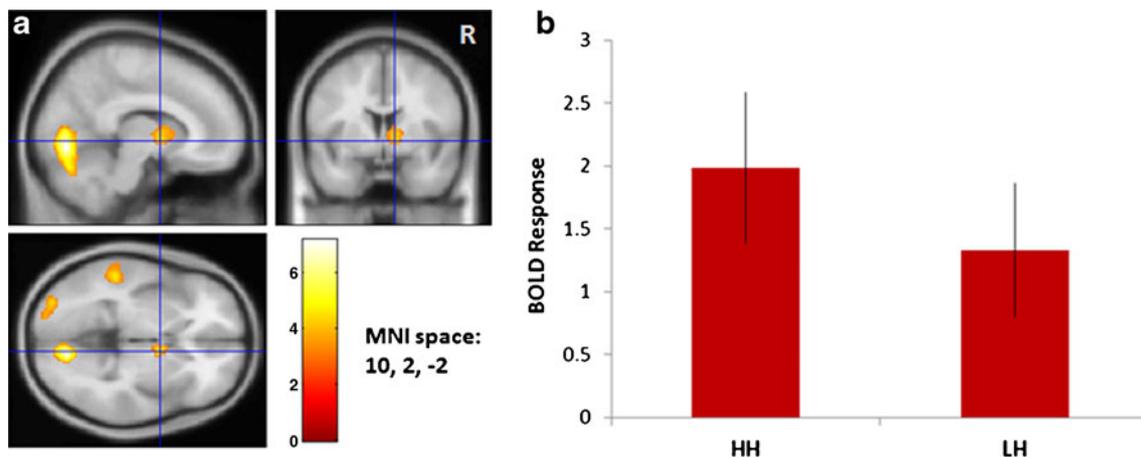

Fig. 3 Greater BOLD response for high-harm as compared to low-harm conditions, collapsed across formats and risk. (a) BOLD activation map in a location most consistent with the right bed nucleus of the stria terminalis (BNST). The color bar represents t statistics. (b) BOLD responses for high-harm (HH) and low-harm (LH) conditions, each relative to the fixation baseline. Both conditions showed increased BOLD signal relative to fixation in the BNST, with higher responses for the high-harm conditions. Beta weights were calculated from 253 voxels that passed a p < .001 voxel-level threshold and p < .05 whole-brain significance, with peak voxel at 10, 2, –2. Error bars represent standard errors of the means
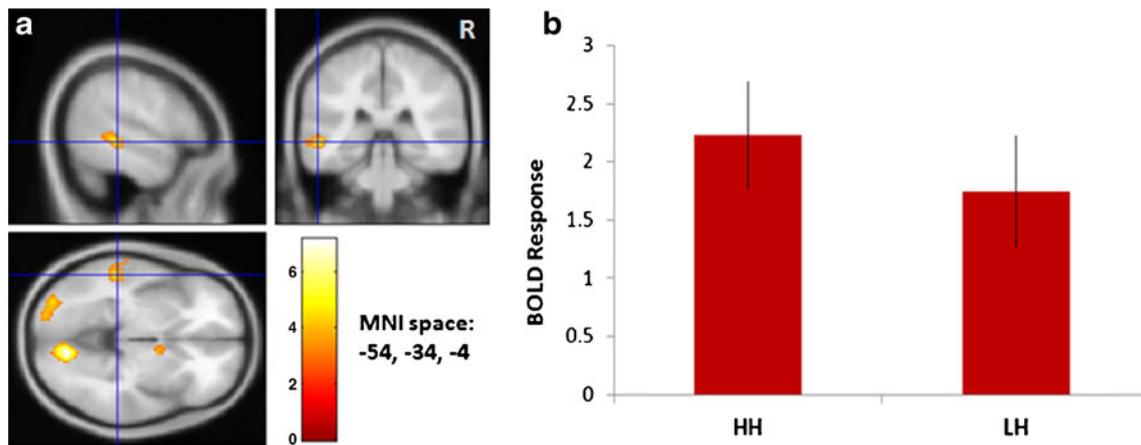
Fig. 4 Greater BOLD response for high-harm as compared to low-harm conditions, collapsed across formats and risk. (**a**) BOLD activation map in the left middle temporal gyrus (MTG). The color bar represents *t* statistics. (**b**) BOLD response for high-harm (HH) and low-harm (LH) conditions, each relative to the fixation baseline. Both conditions showed increased BOLD signal relative to fixation in this region, with the response being higher in the high-harm condition. Beta weights were calculated from 234 voxels that passed a $p < .001$ voxel-level threshold and $p < .05$ whole-brain significance, with peak voxel at −54, –34, –4. Error bars represent standard errors of the means

gyrus showed robust activation. Subcortically, a region bordering the ventral caudate/nucleus accumbens also showed a strong response for the high-risk condition (Fig. 8). No brain regions showed significant activation for the main effect of risk where low-risk were compared to high-risk conditions.

BOLD activity in the VLPFC and the preSMA also showed a Risk x Format interaction, in which the frequency format for high-risk conditions demonstrated robust activations (Table 3). On the other hand, a cluster of cortical, brain-stem, and striatal brain regions showed an interaction in the probability format for the high-risk condition (Table 3). This cluster included middle frontal gyri extend-

ing into the posterior orbital gyrus, along with subcortical midbrain and globus pallidus.

BOLD correlations with behavioral ratings of risk

Since a format bias (greater risk perception in the frequency format) was noted in the behavioral literature, we sought to identify the neural substrates underlying this bias by correlating differences in participant risk ratings in each scenario with their differential BOLD response for each format. The difference between each participant's mean probability- and mean frequency-
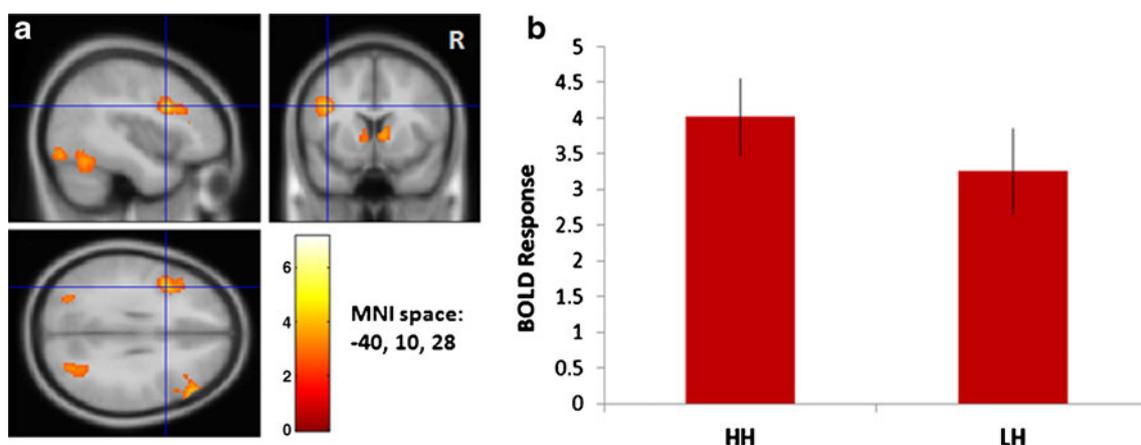

Fig. 5 Greater BOLD response for high-harm as compared to low-harm conditions, collapsed across formats and risk. (**a**) BOLD activation map in the left inferior frontal gyrus pars opercularis (IFG pars opercularis). The color bar represents *t* statistics. (**b**) BOLD response for high-harm (HH) and low-harm (LH) conditions, each relative to the fixation baseline. Both conditions showed increased BOLD signal relative to fixation in this region, with the response being higher in the high-harm condition. Beta weights were calculated from 913 voxels that passed a $p < .005$ voxel-level threshold and $p < .05$ whole-brain significance, with peak voxel at −40, 10, 28. Error bars represent standard errors of the means

Table 2 Brain regions showing greater average BOLD response for low-harm as compared to high-harm conditions

Region	Hemisphere	MNI Space Coordinates			Number of Activated Voxels	t (peak voxel)	p (voxel level)	p (whole brain)
		x	y	z				
Low Harm > High Harm								
Parietal operculum	R	54	–26	24	511	4.25	p < .005	p ≤ .052
Probability Low Harm > High Harm								
Visual cortex	L	–8	–84	18	360	5.02	p < .001	p ≤ .006
Visual cortex	L	–14	–70	–14	238	5.00	p < .001	p ≤ .036
Paracentral lobule	R	8	–38	58	695	4.06	p < .005	p ≤ .013

The number of activated voxels shown is based on a cluster-wise thresholding criterion for each voxel, corrected for multiple comparisons across the whole brain.

format risk ratings was calculated across risk and harm scenario categories (i.e., a positive rating number indicated that the probability format was rated higher than the frequency format). This established an index of sensitivity toward a certain format. Overall, participants tended to rate risks higher in the frequency format than in the probability format, consistent with our behavioral results and prior data. These risk ratings were used as a regressor of interest in a whole-brain analysis of the main format contrasts (probability vs. frequency), corrected for multiple comparisons using a cluster-corrected threshold criterion. There was a significant positive association

between the rating bias and the extent to which probability format produced greater BOLD responses than frequency format in the ventromedial prefrontal cortex (VMPFC; Fig. 9), indicating that the greater the sensitivity toward the probability format, the higher the BOLD activation in the VMPFC. We further tested whether this correlation was driven by reaction time differences between format conditions. We found no significance in this correlation, suggesting that the BOLD sensitivity toward format was more strongly modulated by the risk rating score than by the time taken to reach a decision regarding the risk rating.

Table 3 Brain regions showing greater average BOLD response for high-risk as compared to low-risk conditions

Region	Hemisphere	MNI Space Coordinates			Number of Activated Voxels	t (peak voxel)	p (voxel level)	p (whole brain)
		x	y	z				
High Risk > Low Risk								
Ventrolateral prefrontal	L	–48	28	10	1,541	6.00	p < .001	p < .001
PreSMA	Midline	–6	40	54	1,992	5.33	p < .001	p < .001
Middle/Superior frontal gyrus	L	–44	12	36	310	4.01	p < .001	p ≤ .013
Visual cortex	R	12	–76	–6	604	4.57	p < .001	p < .001
Parietal lobe/White matter	L	–26	–48	32	770	4.06	p < .005	p ≤ .007
Ventral caudate/ Nucleus accumbens	R	10	10	0	1,025	4.10	p < .005	p < .001
Frequency High Risk > Low Risk								
Ventrolateral prefrontal	L	–48	28	10	285	4.50	p < .001	p ≤ .018
PreSMA	Midline	–6	40	54	258	4.44	p < .001	p ≤ .027
Probability High Risk > Low Risk								
Middle frontal gyrus	L	–34	48	14	1,082	4.84	p < .001	p < .001
Middle frontal gyrus	L	–42	26	34	360	4.51	p < .001	p ≤ .006
Posterior orbital gyrus	L	–24	32	–20	216	4.72	p < .001	p ≤ .051
Cerebellum/Visual cortex	R	16	–78	–22	578	4.55	p < .001	p < .001
Midbrain	L	–10	–24	–10	266	4.21	p < .001	p ≤ .024
Globus pallidus	L	–12	–2	4	654	3.80	p < .005	p ≤ .017

The number of activated voxels shown is based on a cluster-wise thresholding criterion for each voxel, corrected for multiple comparisons across the whole brain
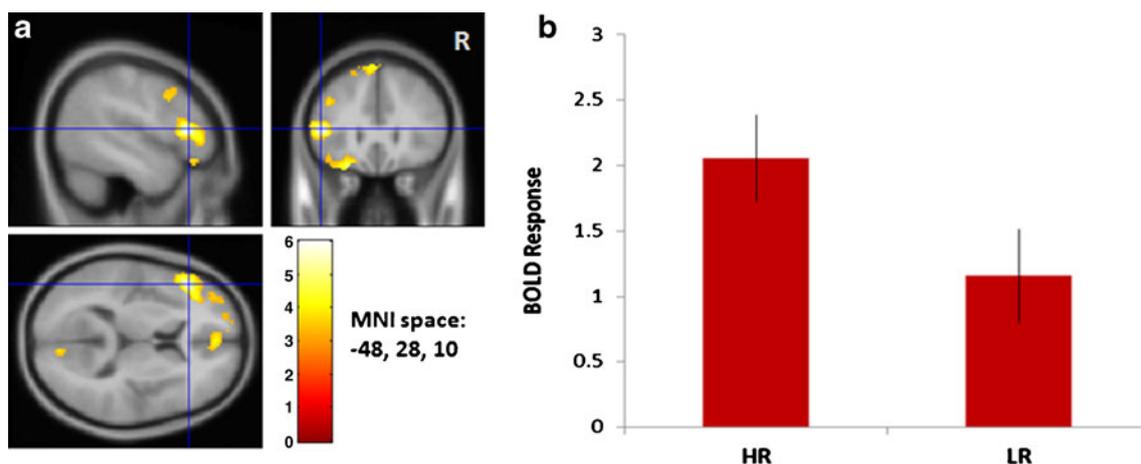
Fig. 6 Greater BOLD response for high-risk as compared to low-risk conditions, collapsed across formats and harm. (**a**) BOLD activation map in the left ventrolateral prefrontal cortex (VLPFC). The color bar represents *t* statistics. (**b**) BOLD response for the high-risk (HR) and low-risk (LR) conditions, each relative to the fixation baseline. High-risk conditions showed increased BOLD signal relative to fixation in these regions. Beta weights were calculated from 1,541 voxels that passed a *p* < .001 voxel-level threshold and *p* < .05 whole-brain significance, with peak voxels at −48, 28, 10. Error bars represent standard errors of the means

Discussion

The present study of risk decisions about physical harms indicates that distinct brain regions are sensitive to qualitative (harm severity) and quantitative (frequency, probability) assessments of risk. Manipulation of the qualitative (presumably affective) characteristics of risk engaged the region of the BNST, frontal cortices, and language-processing areas, while a widespread frontal network of regions along with the ventral striatum were sensitive to the quantitative information within risk assessment. Specific numerical formats (frequency or probability) differentially modulated responses for both harm severity and risk likelihood conditions.

Qualitative assessment of risk

Different brain regions were uniquely sensitive to the qualitative features of risk (severity of harm in risk decisions), since high-harm scenarios in our study revealed BOLD activations for presumably affective components of risk processing. In the present study, high-harm conditions activated an area consistent with the BNST, a region previously shown in anticipatory anxiety for phobia-relevant stimuli (Straube, Mentzel, & Miltnera, 2007). In these conditions, the participants were presented with scenarios that had severe and sometimes fatal harms (breaking several ribs, drowning, and paralysis). The evaluation of risk in such contexts could trigger anxiety,
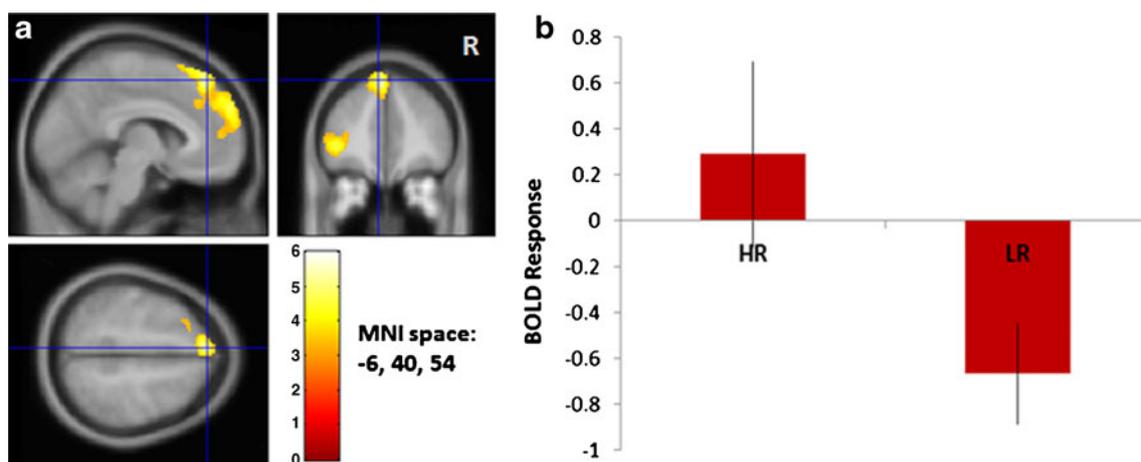

Fig. 7 Greater BOLD response for high-risk as compared to low-risk conditions, collapsed across formats and harm. (**a**) BOLD activation map in the presupplementary motor area (preSMA). The color bar represents *t* statistics. (**b**) BOLD response for the high-risk (HR) and low-risk (LR) conditions, each relative to the fixation baseline. High-risk conditions showed increased BOLD signal relative to fixation in these regions. Beta weights were calculated from 1,992 voxels that passed a *p* < .001 voxel-level threshold and *p* < .05 whole-brain significance, with peak voxels at −6, 40, 54. Error bars represent standard errors of the means
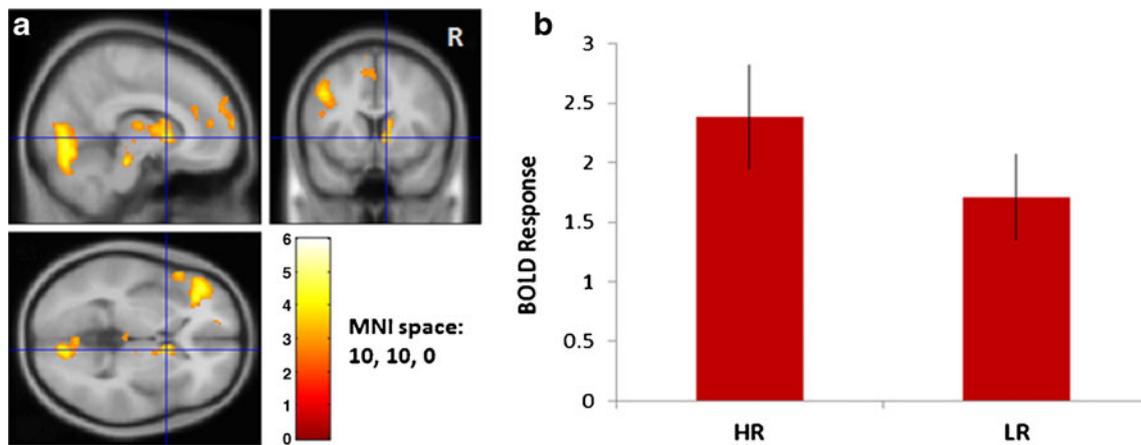
Fig. 8 Greater BOLD response for high-risk as compared to low-risk conditions, collapsed across formats and harm. (a) BOLD activation map in the right ventral caudate/nucleus accumbens. The color bar represents *t* statistics. (b) BOLD response in the midbrain for high-risk (HR) and low-risk (LR) conditions, each relative to the fixation baseline. Both conditions showed increased BOLD signal relative to fixation in the midbrain, with the response being higher for the high-risk conditions. Beta weights were calculated from 1,025 voxels that passed a $p < .005$ voxel-level threshold and $p < .05$ whole-brain significance, with peak voxels at 10, 10, 0. Error bars represent standard errors of the means

as the participants imagine engaging in the high-harm activity and anticipate potential injuries.

Other limbic areas, like the amygdala (which has strong connections with the BNST), orbitofrontal cortex, insula, anterior cingulate, and VMPFC, which are known to be involved in arousal, fear perception, and memory associated with harms, were not significantly activated in the high-harm as compared to low-harm conditions. The absence of BOLD responses in the broader limbic and paralimbic circuitry is surprising, given the aversive nature of the stimuli and the previous neuroimaging results shown by Vorhold and colleagues on the judgment of risk (Vorhold et al., 2007). It is likely that the act of considering a hypothetical scenario and rating the risk of continuing to engage in a physical activity

may be more emotionally detached than a direct evaluation of the participant's degree of fear in engaging in an activity. The implication that evaluative judgment processing can dampen limbic responses has been previously shown in a study where affective responses in the amygdala were disrupted with increased neural activity in the right VLPFC during an affect-labeling task (Lieberman et al., 2007). Although the VLPFC is not known to have direct connections with the amygdala, it has projections to the medial prefrontal cortex, an area that has dense projections to the amygdala (Ghashghaei & Barbas, 2002; Groenewegen, Wright, & Uylings, 1997; McDonald, Mascagni, & Guo, 1996) and is known to inhibit amygdala responses (Quirk, Likhtik, Pelletier, & Paré, 2003; Taylor, Phan, Decker, & Liberzon, 2003). The findings from these
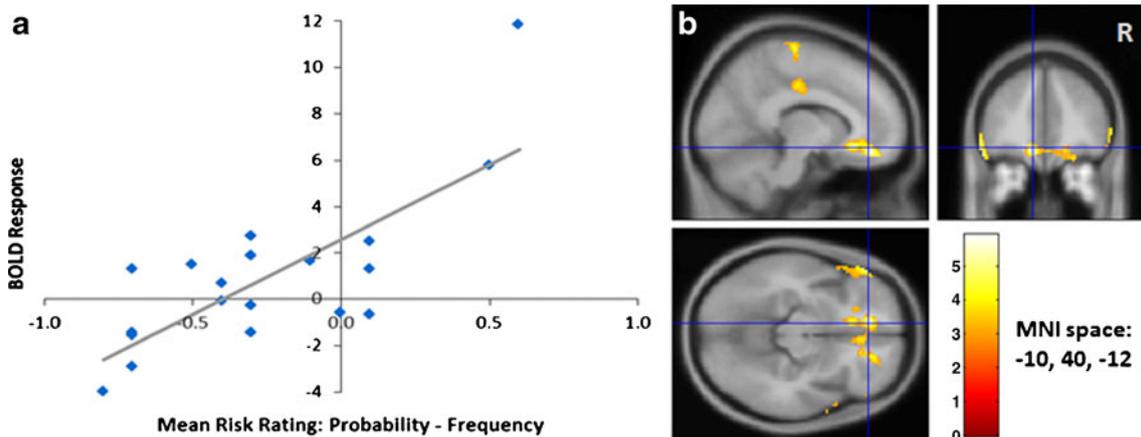

Fig. 9 Correlations of behavioral risk response ratings with fMRI data. (a) Correlation plot of BOLD responses for the probability-format versus frequency-format contrast, showing significant correlation with the behavioral risk response ratings across participants in the ventromedial prefrontal cortex (VMPFC). Peak activation voxel, –10, 40, –12; cluster size = 761; voxel-level threshold, $p < .005$; whole-brain p value < .003, corrected for multiple comparisons; peak voxel z value = 5.92. Blue diamonds represent the spread of individual scores with the line of best fit. (b) BOLD activation map in the VMPFC. The color bar represents t statistics

studies offer a potential explanation for the loss of limbic activity seen in the present research. We observed a robust VLPFC activation for high-risk conditions and IFG pars opercularis activation for high-harm conditions, and both of these areas may be contributing to the diminished emotional response seen within limbic brain regions in our study. Anecdotally, during post-experimental briefing sessions a number of participants claimed that the harms associated with the physical activities presented would not, in reality, happen to them. These individuals had a lower perception of risk and subsequently reported a lower risk rating, alluding to the possible loss in observed neural activity in the limbic regions. In order to rule out the effects of habituation in these areas across the eight runs, we contrasted neural activity in the first four and the last four runs. No significant evidence of habituation was observed in limbic or paralimbic circuits.

The patterns of BOLD activation in areas involved in language processing suggest a potential unique involvement of language regions in risk encoding, at least when the information is derived from verbal cues. Our data showed a significant activation for high-harm conditions in the left MTG, an area that has been reported in previous neuro-imaging studies to play a role in processing the semantic aspects of words (content words vs. function words; see Diaz & McCarthy, 2009). In comparison to low-harm conditions, the verbal semantics of assessing harm severity content in the high-harm conditions in our study seemed to elicit a strong response in the MTG. Additionally, the complex linguistic processing necessary for evaluating the severity of harm in these scenarios seemed to recruit other cortical language-processing areas such as the IFG and the angular gyrus. There has been evidence showing that these areas, especially the IFG pars opercularis, are engaged in inference processing for inferring the intention of a human character or the physical consequence of an action (Mason & Just, 2011). The right middle frontal gyrus (MFG) also showed significant activation for high-harm conditions, an area that has been elicited in lexical decision-making tasks for reading words in a word-like context as compared to a non-word-like context (Newman & Joanisse, 2011). Understanding the context of a situation is an important consideration in the risk assessment process, and the right MFG could play a role in comprehending the context as textual information is being read in the high-harm scenarios. Thus, the involvement of such a frontal cortical network in our study for high-severity conditions could be indicative of complex language comprehension required for processing the textual content, as well as inference strategies necessary for evaluating the physical consequences of engaging in a risky activity.

Overall, we observed that when severe harm conditions are presented (irrespective of risk level and format of representation), cortical regions primarily facilitate language comprehension (reading, semantic processing, and making inferences), while the subcortical BNST shapes the affective characteristics involved in the qualitative assessment of risk. When format was considered, we noted that a majority of the brain areas reported in the high-harm versus low-harm contrast were primarily driven by an interaction effect in the frequency format. From prior behavioral studies, it is known that the frequency format elicits a higher perception of risk than does the probability format for equivalent harm contexts (Siegrist, 1997; Slovic et al., 2000; Yamagishi, 1997). Our fMRI data validate these behavioral findings, suggesting that the frequency format may play an important role in influencing risky decision making, at least in the context of severe physical injury. The high-harm conditions in the probability format did not elicit such a robust response.

Quantitative assessment of risk

Aside from processing the qualitative characteristics of risk decisions, the data indicated that higher order cognitive areas within the frontal lobe were particularly sensitive to quantitative aspects (the likelihood of injury) of risk processing. Specifically, high-risk conditions compared to low-risk conditions engaged a network of regions in the frontal lobe with peak activations in the preSMA, the VLPFC and the middle/superior frontal gyrus (MFG/SFG). The collective activation of these brain regions suggests that different parts of the frontal cortex may be individually sensitive to the processing of different phases of risk assessment in the high-risk condition.

The preSMA has been previously shown as a region involved in appropriating strategies and in signaling mismatch of strategies (Muhammad, Wallis, & Miller, 2006; Wolfensteller & von Cramon, 2010), so it could be involved in two different neural processes in the present study. First, the preSMA may function to determine the type of strategy to use in the assessment of risk (e.g., computational strategies for calculating the numerical value of the risk, linguistic strategies for the purpose of examining the semantic meaning of the scenarios, or strategies for evaluating the severity of the harm and estimating the perceived likelihood of the harm). Second, this area may be involved in flagging a conflict of strategies as the participant tries to decide whether to use the likelihood level or the harm level, or both, to assess the risk. Therefore, the preSMA region in the present study may be involved in modulating the decision criteria for the type of strategy used to evaluate risk in the task.

We observed a strong response within the left VLPFC, an area previously shown to be activated for conflict associated with cognitive as compared to affective tasks (Ochsner, Hughes, Robertson, Cooper, & Gabrieli, 2009). In the present study, this area may be involved in signaling

tasks that demand competing cognitive resources. High-risk conditions require the participants to evaluate risk by estimating the level of harm (extent of injury incurred, threat, recovery time) and the likelihood of the harm occurring, both of which need to be assessed at the same time, thereby increasing cognitive load. Hence, a decision for rating risks in a high-likelihood risk condition may be more cognitively demanding than a decision in a low-likelihood risk condition.

Beyond the cognitive processes that mediate risk assessment, computational and anticipatory mechanisms likely shape an individual's risk preference (to be risk averse or risk seeking). Our data showed BOLD activations in the ventral caudate/nucleus accumbens for the high-risk conditions. The caudate has been reported in the monetary risk assessment literature as differentially encoding gains and losses (Seymour, Daw, Dayan, Singer, & Dolan, 2007), characterizing expected reward and reward variance reflecting risk (Preuschoff, Bossaerts, & Quartz, 2006), and being active during risk conditions as compared to ambiguous conditions (Hsu et al., 2005). Other neuroeconomics studies have shown the nucleus accumbens to be involved in the anticipation and prediction of gains (Knutson, Adams, Fong, & Hommer, 2001; Kuhnen & Knutson, 2005). Although the scenarios presented in our study do not have a rewarding component, the characterization of expected value in each situation (combining the likelihood of risk with the severity of the physical injury) and the encoding of losses/aversive consequences (presumably associated with physical injury) seem to engage the ventral caudate area. Additionally, anticipation of potential injury produced while evaluating high-risk conditions could explain the involvement of the nucleus accumbens.

In the Risk x Format interaction, we observed strong activations in the middle and prefrontal gyri for the probability format in high-risk conditions. The left MFG has been associated with decreased distractor interference in attentional-learning paradigms (Kelley & Yantis, 2010), where following training, distractors elicited fewer responses in the MFG. Additionally, in situations demanding inference processing, the left MFG has been shown to be associated with coherence monitoring, a cognitive process engaged to ensure that the flow of information between sentences is cohesive and comprehensible (Mason & Just, 2011). In the present context, one might speculate that the left frontal areas play a role in actively sorting and filtering pertinent information (such as likelihood of risk and severity of harm) from the scenarios. Thus, the activation of the left frontal regions in the high-risk conditions primarily in response to the probability format suggests that the evaluation of risk in these settings is more cognitively demanding in comparison to the same condition in the frequency format. This result is consistent with evolutionary theories of risk assessment (Gigerenzer, 1998; Jones & Goldsmith, 2005). Anecdotally, in post-experimental

briefing sessions, the participants stated that the evaluation of risk in the probability format (decimal numerical representation) was more mentally strenuous than in the frequency format (ratio numerical representation), because they had to convert the decimal representation into a percentage format and then combine the severity of harm and the likelihood of risk in order to make a decision regarding the risk rating.

The midbrain also showed a robust response in this probability-format high-risk interaction effect. The midbrain has been previously reported for processing novel salient stimuli (Krebs, Schott, & Düzel, 2009) and for voluntary risk-taking choice behavior in the balloon assessment risk task (Rao, Korczykowski, Pluta, Hoang, & Detre, 2008). In our study, the midbrain area may be involved in processing novelty with regard to the scenarios or motivation associated with making a decision. Even though our stimuli did not strictly control for novelty (four different physical activities were randomly presented), the combination of the physical activity, risk likelihood, and harm type was unique to each scenario. These combinations of risk scenarios in the probability high-risk conditions could be characterized as being more novel and salient than those in comparable low-risk conditions and, as a result, could engage the midbrain. Moreover, motivational cues represented in the midbrain could reflect an additional level of attentiveness and effort required for processing high-risk conditions in the probability format.

Format of risk communication affecting risk assessment

We did not observe a main effect of format, so we investigated whether the BOLD responses in the format contrast (probability vs. frequency) correlated with the behavioral risk ratings of the participants. As predicted, most participants showed a bias for perceiving greater risk when information was presented in the frequency format. The participant's sensitivity to this bias was associated with the level of activation in the VMPFC. Specifically, participants who showed less of this bias, or even a reverse bias, showed greater engagement of the VMPFC. This finding parallels the rationality index developed by De Martino and colleagues (De Martino, Kumaran, Seymour, & Dolan, 2006), in which participants who were less biased by framing effects demonstrated enhanced VMPFC activity during decision making. Thus, the VMPFC appears critical in the ability to overcome classic decision-making biases.

Comparison with other risk neuroimaging studies

While most neuroimaging literature on risk has investigated brain regions involved with monetary risk, their results cannot be fully extended to explain our fMRI findings. One difficulty in comparing risk studies is the substantially

different design methodologies used to present stimuli, as well as the varying definitions of risk across fields. Weber and colleagues (Weber, Blais, & Betz, 2002), in their psychometric scale for risk assessment, found that individuals are not consistent in their risk-taking attitudes across domains, such as financial, health/safety, recreation, ethical, and social decision making. Given these varied definitions of risk and risk-taking attitudes, it is likely that distinct cognitive mechanisms are engaged during risk evaluations in different domains, and therefore clear and differentiated stimulus contingencies would be necessary to probe the neural substrates underlying risk in these different domains.

In conclusion, the present findings and the aforementioned studies reveal that decision making involving risk is an inherently complicated task, with distinct regions of the brain being sensitive to different aspects of risk processing. Within the domain of assessing risks of aversive consequences with regard to physical injury, different cortical and subcortical networks were employed. When evaluating the high severity of harm, cognitive resources were used for reading, language comprehension, and interpretation of anxiety associated with the harm, processes reflecting qualitative features of risk assessment. On the other hand, when evaluating a high likelihood of risk, cognitive demands were focused for computation and inference of relevant risk information, for modulating various decision strategies, and for resolving conflict associated with decision making, processes all comprising the quantitative features of risk assessment. By manipulating the harm level, the risk likelihood level, and the format of risk communication, we were able to successfully identify the neural substrates of risk assessment associated with physical harm.

References

De Martino, B., Kumaran, D., Seymour, B., & Dolan, R. J. (2006). Frames, biases, and rational decision-making in the human brain. *Science, 313,* 684–687. doi:10.1126/science.1128356.

Diaz, M. T., & McCarthy, G. (2009). A comparison of brain activity evoked by single content and function words: An fMRI investigation of implicit word processing. *Brain Research, 28,* 38–49.

Ghashghaei, H. T., & Barbas, H. (2002). Pathways for emotion: Interactions of prefrontal and anterior temporal pathways in the amygdala of the rhesus monkey. *Neuroscience, 115,* 1261–1279.

Gigerenzer, G. (1998). Ecological intelligence: An adaptation for frequencies. In D. D. Cummins & C. Allen (Eds.), *The evolution of mind* (pp. 9–29). New York: Oxford University Press.

Groenewegen, H. J., Wright, C. I., & Uylings, H. B. (1997). The anatomical relationships of the prefrontal cortex with limbic structures and the basal ganglia. *Journal of Psychopharmacology, 11,* 99–106.

Hsu, M., Bhatt, M., Adolphs, R., Tranel, D., & Camerer, C. F. (2005). Neural systems responding to degrees of uncertainty in human decision-making. *Science, 310,* 1680–1683. doi:10.1126/science.1115327.

Jones, O. D., & Goldsmith, T. H. (2005). Law and behavioral biology. *Columbia Law Review, 105,* 405–502.

Kahneman, D., & Tversky, A. (1979). Prospect theory: An analysis of decision under risk. *Econometrica, 47,* 263–291.

Kelley, T. A., & Yantis, S. (2010). Neural correlates of learning to attend. *Frontiers in Human Neuroscience, 4,* 1–11.

Koehler, J. J. (2001). The psychology of numbers in the courtroom: How to make DNA match statistics seem impressive or insufficient. *Southern California Law Review, 74,* 1275–1306.

Knutson, B., Adams, C. M., Fong, G. W., & Hommer, D. (2001). Anticipation of increasing monetary reward selectively recruits nucleus accumbens. *Journal of Neuroscience, 21,* RC159.

Krebs, R. M., Schott, B. H., & Düzel, E. (2009). Personality traits are differentially associated with patterns of reward and novelty processing in the human substantia nigra/ventral tegmental area. *Biological Psychiatry, 65,* 103–110. doi:10.1016/j.biopsych.2008.08.019.

Kuhnen, C. M., & Knutson, B. (2005). The neural basis of financial risk taking. *Neuron, 47,* 763–770.

Lieberman, M. D., Eisenberger, N. I., Crockett, M. J., Tom, S. M., Pfeifer, J. H., & Way, B. M. (2007). Putting feelings into words: Affect labeling disrupts amygdala activity in response to affective stimuli. *Psychological Science, 18,* 421–428. doi:10.1111/j.1467-9280.2007.01916.x.

Mason, R. A., & Just, M. A. (2011). Differentiable cortical networks for inferences concerning people's intentions versus physical causality. *Human Brain Mapping, 32,* 313–329. doi:10.1002/hbm.21021.

McDonald, A. J., Mascagni, F., & Guo, L. (1996). Projections of the medial and lateral prefrontal cortices to the amygdala: A *Phaseolus vulgaris* leucoagglutinin study in the rat. *Neuroscience, 71,* 55–75. doi:10.1016/0306-4522(95)00417-3.

Muhammad, R., Wallis, J. D., & Miller, E. K. (2006). A comparison of abstract rules in the prefrontal cortex, premotor cortex, inferior temporal cortex, and striatum. *Journal of Cognitive Neuroscience, 18,* 974–989. doi:10.1162/jocn.2006.18.6.974.

Newman, R. L., & Joanisse, M. F. (2011). Modulation of brain regions involved in word recognition by homophonous stimuli: An fMRI study. *Brain Research, 1367,* 250–264.

Ochsner, K. N., Hughes, B., Robertson, E. R., Cooper, J. C., & Gabrieli, J. D. E. (2009). Neural systems supporting the control of affective and cognitive conflicts. *Journal of Cognitive Neuroscience, 21,* 1841–1854. doi:10.1162/jocn.2009.21129.

Phillips, R. G., & LeDoux, J. E. (1992). Differential contribution of amygdala and hippocampus to cued and contextual fear conditioning. *Behavioral Neuroscience, 106,* 274–285. doi:10.1037/0735-7044.106.2.274.

Preuschoff, K., Bossaerts, P., & Quartz, S. R. (2006). Neural differentiation of expected reward and risk in human subcortical structures. *Neuron, 51,* 381–390.

Quirk, G. J., Likhtik, E., Pelletier, J. G., & Paré, D. (2003). Stimulation of medial prefrontal cortex decreases the responsiveness of central amygdala output neurons. *Journal of Neuroscience, 23,* 8800–8807.

Rao, H., Korczykowski, M., Pluta, J., Hoang, A., & Detre, J. A. (2008). Neural correlates of voluntary and involuntary risk taking in the human brain: An fMRI study of the balloon analog risk task (BART). *NeuroImage, 42,* 902–910.

Seymour, B., Daw, N., Dayan, P., Singer, T., & Dolan, R. (2007). Differential encoding of losses and gains in the human striatum. *Journal of Neuroscience, 27,* 4826–4831. doi:10.1523/JNEUROSCI.0400-07.2007.

Siegrist, M. (1997). Communicating low risk magnitudes: Incidence rates expressed as frequency versus rates expressed as probability. *Risk Analysis, 17,* 507–510.

Slovic, P., Monahan, J., & MacGregor, D. G. (2000). Violence risk assessment and risk communication: The effects of using actual cases, providing instruction and employing probability verses frequency formats. *Law and Human Behavior, 24,* 271–296.

Straube, T., Mentzel, H. J., & Miltnera, W. H. R. (2007). Waiting for spiders: Brain activation during anticipatory anxiety in spider phobics. *NeuroImage, 37,* 1427–1436.

Taylor, S. F., Phan, K. L., Decker, L. R., & Liberzon, I. (2003). Subjective rating of emotionally salient stimuli modulates neural activity. *NeuroImage, 18,* 650–659.

Tobler, P. N., O'Doherty, J. P., Dolan, R. J., & Schultz, W. (2007). Reward value coding distinct from risk attitude-related uncertainty coding in human reward systems. *Journal of Neurophysiology, 97,* 1621–1632.

Viscusi, W. K., & Evans, W. (1990). Utility functions that depend on health status: Estimates and economic implications. *American Economic Review, 80,* 353–374.

Vorhold, V., Giessing, C., Wiedemann, P. M., Schütz, H., Gauggel, S., & Fink, G. R. (2007). The neural basis of risk ratings: Evidence from a functional magnetic resonance imaging (fMRI) study. *Neuropsychologia, 45,* 3242–3250. doi:10.1016/j.neuropsychologia.2007.06.023.

Walton, M. E., Croxson, P. L., Behrens, T. E. J., Kennerley, S. W., & Rushworth, M. F. S. (2007). Adaptive decision making and value in the anterior cingulate cortex. *NeuroImage, 36,* T142–T154.

Weber, E. U., Blais, A.-R., & Betz, N. E. (2002). A domain-specific risk-attitude scale: Measuring risk perceptions and risk behaviors. *Journal of Behavioral Decision Making, 15,* 263–290.

Wolfensteller, U., & von Cramon, D. Y. (2010). Bending the rules: Strategic behavioral differences are reflected in the brain. *Journal of Cognitive Neuroscience, 22,* 278–291.

Yamagishi, K. (1997). When a 12.86% mortality is more dangerous than 24.14%: Implications for risk communication. *Applied Cognitive Psychology, 11,* 495–506. doi:1.1002/(SICI)1099-0720(199712)11:6<495::AID-ACP481>3.CO;2-J.